Design of a Freeze Plug for the Molten Salt Reactor (MSR)

Parth Swaroop
4412826

Friday 18th September, 2015

System Integration Project (SIP) - II (SET3811)

Supervisor:
Dr. ir. M. Rohde
Prof. Dr.ir.Jan Leen Kloosterman

Section of Nuclear Energy and Radiation Applications
Department of Radiation Science and Technology
Faculty of Applied Science
Delft University of Technology

Contents

List of Figures

List of Tables

Abstract

In this report, the design of a freeze plug which is one of the safety component in generation IV Molten Salt Reactor (MSR), is studied. From the experience of Fukushima-Daiichi nuclear power plant disaster, it is preferred to remove the decay heat from reactor core, passively i.e without mechanical or electrical assistance. This decay heat calculation is adopted from [16] but rest of the engineering aspects of the freeze plug with respect to the current MSR design is unknown. Further the solid properties of salt $LiF - ThF_4$ $(78\% - 22\%)$ used in the MSR, is unknown. Hence the reactor core with a freeze plug system is studied using water/ice data. A simplified model with a rectangular cross section of freeze plug is adopted to study the heat transfer from reactor core to plug. The mathematical model initially formulated with decay heat comprising of a moving interface and time dependant boundary condition is too complex to establish preliminary understanding. This is further simplified to a constant temperature boundary condition with moving interface and conduction as dominant heat transfer for which the analytical solution is available. These analytical results are compared with experiment performed by Ramazan Kahraman et al. [9]. The results show very large melting times in absence of heat source. Also, interface position curve for pure conduction model deviates from the experimental results in which convective effects are also dominant. Further, sensitivity analysis is performed which shows strong dependence of interface position on thermal conductivity and latent heat of fusion.

Chapter 1

Introduction

In 2011, the Fukushima-Daiichi nuclear power plant suffered from the natural disaster of the great-east Japan Earthquake and subsequently followed by tsunami. Although the reactors was designed to be protected against emergency situations, based on previous scientific data available [15], the natural disaster still managed to inflict a significant damage to the power plant.

After the earthquake, due to the loss of external power source, the reactors units were shutdown. Despite shutdown, the reactor cores were still be producing about a few percent of their nominal thermal power, from fission product decay [18]. The external cooling circuit which includes the cooling pumps and the heat exchanger, dumped the reactor heat into the sea. This system was running on back-up generators to remove the residual heat from the core during the external power loss. Earthquake was followed by tsunami, which eventually submerged the back-up power system, leading to the failure of the auxiliary cooling system. Ultimately, it isolated the reactor cores from their heat sink, causing the fuel to melt.

This incident has been translated into an important safety requirement for the future nuclear reactor system. The system has to be passive and effectively remove the decay heat during electrical/mechanical power system failure. The design evaluated in the generation IV Molten Salt Reactor (MSR) for this purpose, is a freeze plug. This idea was carried forward from MSR experiments conducted by ORNL in 1960s because a proven and reliable mechanical valve suitable for the application was unavailable during that time [3]. It will placed in the pipe between the reactor core and the sub-critical drain tanks. It will melt due the decay heat, consequently allowing the fuel to be drained in the sub-critical storage tanks. This report studies the design of a freeze plug for the MSR.

1.1 Overview of Molten Salt Reactor

MSR are referred to a class of nuclear fission reactors in which fissile material is dissolved in the molten salt. This fuel is typically fissile material such as UF_4, PuF_3, minor actinides fluorides and/or fertile elements as ThF_4 depending on the desired application (breeder reactor, actinides burner, etc) dissolved in molten fluoride salt such as LiF , BeF_2 etc [17].

The physical properties of the salt also allow MSRs to run at high temperature which range from 700°C to 750°C) [16] and operate at near atmospheric pressure. MSRs have large negative temperature feedback coefficients. Temperature feedback is the change in the reactivity of the core with the change in temperature. Since the reaction coefficient is negative it allows the reactor to be shut down due to expansion of the fuel salt when temperature increases beyond design limits. These salts are, also relatively inert substances with no rapid reaction with the air or water. Hence there is neither fire nor explosion

hazard for this fuel.

In MSR, fission reactions occur within the mixture of molten salt and liquid fuel. This fuel can be transported between the reactor core and external heat exchanger with the help of a pump and piping system. The heat produced during the reaction is transferred to a secondary clean liquid-salt coolant from the primary molten salt. This configuration is depicted in the figure(1.1). It also consists of a circuit which connects the core volume to the sub-critical storage tanks through a freeze plug. A freeze plug acts like a valve and is a compound of solid state of the fuel salt. In normal operating condition, the solid plug will be cooled with the help of external fan(s) (this is not shown in the figure). During the pump failure (or any other critical scenario in which reactor needs to be stopped), the solid plug begins to melt due the decay heat from the reactor core. After the complete melting of the solid salt, it is possible to drain the fuel salt through gravity.

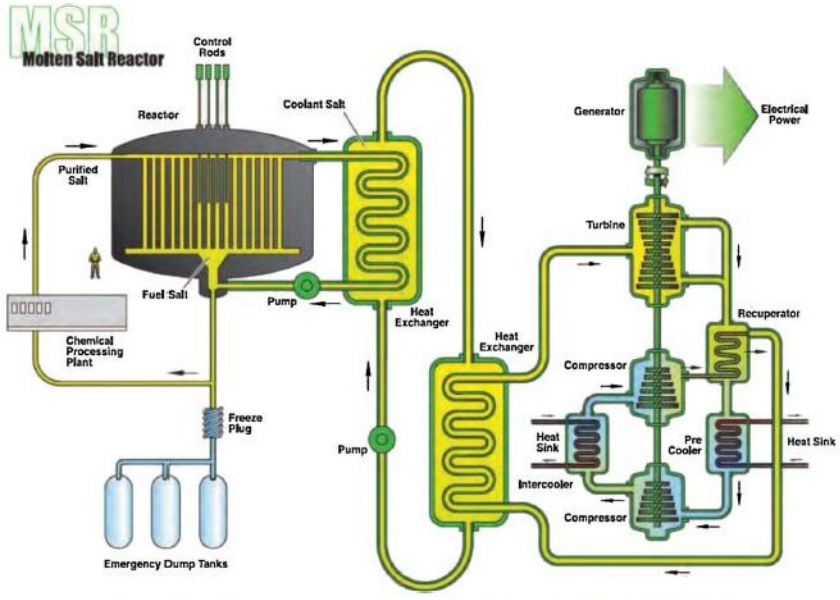

Figure 1.1: A schematic representation of typical MSR design (Generation IV Forum in 2002).

1.2 Design Requirements of the Plug

The reactor model behaviour adopted from [16] is used for the report. Based on simulation, it was predicted that decay heat will be initially 4.3% of the nominal power of the reactor. Since this decay heat is not removed, the reactor core temperature will increase with time. The temperature increase due to the decay heat is represented in shown in fig (1.2). Although the salt boiling point is 2028 K, the damage to reactor system occurs at a earlier temperature of 1473 K which indicates the melting temperature of steel. Hence the safety system is required to drain the fuel before this point is reached. Based on the results, the damage point is reached in approximately 11 minutes, while the boiling point is reached after 30 minutes. Within these 11 minutes, the solid salt has to be melted with the available decay heat and all the molten salt has to be drained into the sub critical tank. Since it does not rely on external electrical or mechanical source , the system is called passive Decay Heat Removal(DHR).

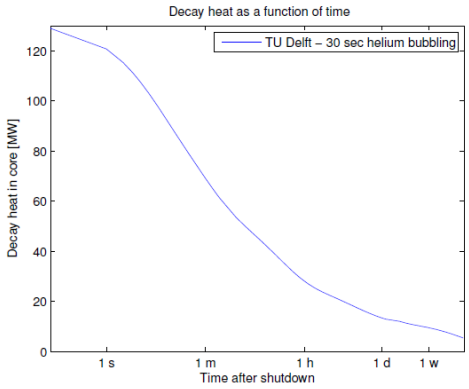

Figure 4.20: **Decay heat as a function of time after shutdown is homogeneously distributed over the salt's volume. Helium bubbling lowers the initial rate.**

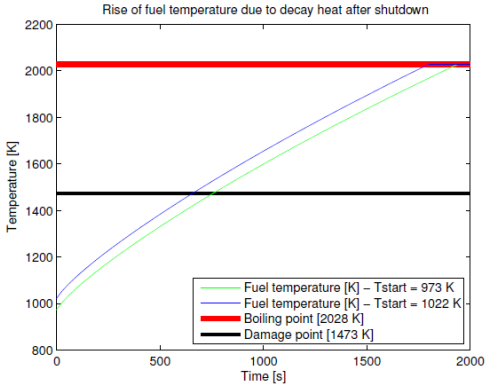

Figure 4.21: **Due to decay heat, the fuel temperature rises from either 973 K (in between the inlet and outlet temperature) or 1022 K, the outlet temperature.**

Figure 1.2: P_{decay} and temperature distribution for the reactor. Adopted from [16]

The following parameters are evaluated as a part of the design of freeze plug:

i Time taken for the salt to melt (t_m);

ii thickness of the salt (δ) ;

iii diameter of the tube (D) ;

iv final flow rate (Φ_v) of the salt to the subcritical drain tanks.

Also, during the normal operating condition, it is required that the plug is fixed despite the weight of the liquid volume above. This requirement will also govern the parameters like thickness, cross-sectional area of the plug and geometry of the pipe. The ultimate aim of the design of freeze plug is to incorporate both mechanical and thermal requirements, but this report is confined only to study the heat transfer between the core and the freeze plug.

Chapter 2

Modelling

2.1 Formulation of the problem

A possible model of a simple rectangular freeze plug is shown in figure(2.1a) to understand the heat transfer phenomena from the reactor core to the plug. The plug should be placed as close to the core as possible in order to extract the maximum decay heat. In figure (2.1b) $x < 0$ represent the liquid fuel salt region from the core while $0 < x \leqslant L$ is the solid plug region. At time (t=0), the initial conditions for the molten fuel salt is temperature ($T_1(t) = 973$ K) which is equal to the reactor temperature. The freeze plug, in solid state, is maintained at temperature $T_2 = 723K$. Also, $(T_1 > T_m > T_2)$, where $(T_m = 858K)$ is the melting temperature. The problem is represented in terms of 1-D heat transfer model.

The phase change process is represented in fig(2.1b) for $t > 0$. In this figure, for any $t > 0$, an amount $\delta(t)$ of salt has already melted. The position of the interface between solid and liquid is identified by the layer with temperature T_m. Thus the liquid temperature decreases from T_1 to T_m while the solid temperature increases from T_2 to T_m. An expected temperature profile is drawn for the process.

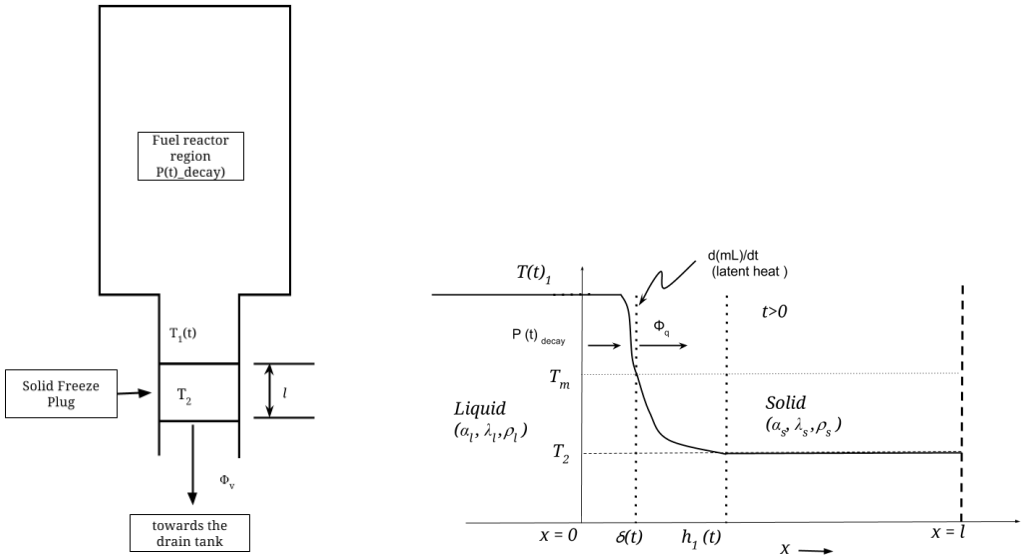

(a) Reactor Core with the Plug

(b) Freeeze plug as the control volume

Figure 2.1: The process of phase change is represented by line diagram in the figure (2.1b). The vertical axis represents the temperature while the horizontal axis represents the length of the plug. At any time $t > 0$ i.e. after the plug has started melting, the interface has moved up to a distance $\delta(t)$ from the initial position x=0.

The process is formulated according to following assumptions:

i Since the problem is represented in 1D, the effects from wall boundaries is neglected. It is also assumed that the plug is uniformly heated i.e melting layer can be represented by a vertical line as shown in fig(2.1b).

ii During the normal operating condition, it is required that plug should be externally cooled to be maintained at T_2. Hence it would be a good approximation to consider its surrounding to be in thermal equilibrium with the plug. Thus, at x=l there would be no temperature exchange with the environment. Therefore, a constant flux can be applied at the boundary position.

iii It is expected that the freeze plug will be a solidified compound of $LiF - ThF_4$ which is the reactor fuel itself. Due to the same fluid and solid composition, it is assumed that the melted liquid from the freeze plug gets instantaneously mixed with the reactor fluid.

iv In order to identify the solid boundary (freeze plug control volume) it is assumed that it will be represented by the interface T=Tm. Also the energy balance (exchange of heat from liquid salt to freeze plug along with latent heat absorption) as a boundary condition will be applied to this layer.

v The heat transfer from the molten salt to the freeze plug takes place by conduction.

Heat conduction can be mathematically represented as below:

$$\frac{\partial T(x,t)}{\partial t} = \alpha \frac{\partial^2 T(x,t)}{\partial x^2} \tag{2.1}$$

where α is the thermal diffusivity (m^2/s) of a material.
Initial Condition:

$$T(x,0) = T_2 \tag{2.2}$$

Boundary Condition:

$$T(x,t)|_{x=\delta} = T_m \tag{2.3}$$

where $\delta(t)$ is the position of the interface. This is followed by insulated boundary condition described by :

$$\left.\frac{\partial T(x,t)}{\partial x}\right|_{x=l} = 0 \tag{2.4}$$

Energy Balance at this interface position ($\delta(t)$):

$$\phi_{in} - \phi_{out} + \text{Production} - \text{Consumption} = \frac{d}{dt}$$

This equation is a generic balance for any quantity. For example it can be applied to mass, momentum or energy, any required parameter of interest. In this case, ϕ_{in} and ϕ_{out} represent the energy inflow and energy outflow at the interface δ respectively. The consumption term at δ is the latent heat of fusion (L), [J/kg] , which is utilized in melting the solid. There is no accumulation of energy at the interface , hence the d/dt term is zero. This is also represented in the figure (2.1b).

$$P_{decay}(t) - \left(-\lambda_s A \left.\frac{\partial T(x,t)}{\partial x}\right|_{x=\delta} \right) - L\frac{dm_s}{dt} = 0$$

The negative sign signifies decrease in the mass of solid (m_s) with increasing time. Substituting,

$$\frac{Ldm_s}{dt} = L\frac{d(\rho_s V)}{dt} = L\frac{d(\rho_s A\delta)}{dt} = L\rho_s A\frac{d\delta}{dt}$$

$$L\rho_s A\frac{d\delta}{dt} = P(t)_{decay} + \lambda_s A\frac{\partial T(x,t)}{\partial x}\bigg|_{x=\delta} \tag{2.5}$$

Here ρ_s and λ_s represent the density and thermal conductivity of the solid salt. These properties (λ, ρ, C_p, L) for solid state of salt are unknown due to lack of experimental results. The physics of heat transfer is thus, studied for the data of water-ice system. Firstly, it is important to note that the salt is a binary system consisting of $LiF - ThF_4$ [2] whereas water/ice is a pure compound.

2.1.1 Phase Change

For a chemical compound, a phase, is defined as a homogeneous, physically distinct, and mechanically separable state of the material, for a given chemical composition. It is a function of both pressure and temperature. The process of phase change behaviour is different for pure crystalline substance and binary compounds. A binary system is a homogeneous mixture of two different substances and their phase changes depends on the solubility of these substance in each other in different phases.

- For a pure substance like water, phase change occurs at constant temperature. The process is depicted in the curve(a) of fig(2.2). Initially heat is removed from a liquid state which results in gradual temperature decrease, until the point B. It is at this point at which first crystal are formed and further removal of heat, equivalent to the latent heat, results in complete solidification (point C) at constant temperature. This Latent heat required is equal to the enthalpy difference at points B and C. Above this, one exception to phase change of ice to water is that the $\rho_w > \rho_w$, where subscript i and w denote ice and water respectively. Hence phase change of water will be associated by volume compression and can lead to convective effects

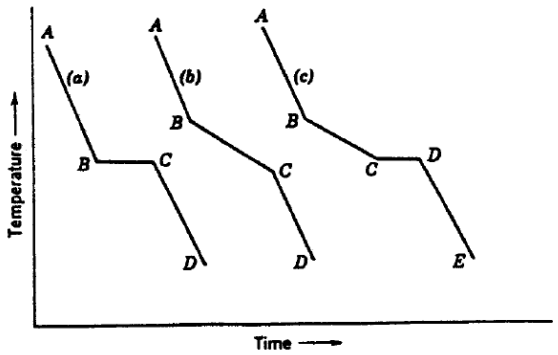

Cooling curves: (a) pure compound; (b) binary solid solution; (c) binary eutectic system.

Figure 2.2: These are cooling curves represent solidification of pure substance (fig(a), binary solid solution(fig (b) and binary eutectic solution (fig (c)). The changes in temperature is observed when the energy is extracted from liquid state various compounds with respect to time. Hence A to B represent liquid state, B to C represent phase change and C to D represent solid. Adopted from [7]

- Further, the curve(b) shows the cooling process of binary system in which are both the substance soluble in liquid as well as solid phases. This melting/freezing range for

binary substance is attributed to the fact that there are changes in the composition of the two substances in the solid and liquid phase.

- The curve(c) shows the cooling of two substance which are completely soluble in liquid state while non-soluble in solid state. Crystallisation starts at point B , where the component with excess composition starts to solidify. At C, the mixture has reached a composition where both start solidifying simultaneously from the liquid solution and temperature remains constant [7]. The fuel salt used in the MSR , would be expected to undergo either (b) or (c) type phase transition.

However it is still convenient to study the overall process using ice as plug because thermal properties and behaviour of water/ice system well known. In case of other compounds, it would be also required to study their reactions and affects in presence of radioactive materials and with fuel salt. Also, various experiments and analytical/numerical models about melting and freezing have been studied for water/ice extensively.

2.1.2 Stefan Number

Based on formulation of problem in section (2.1), heat transfer from the reactor core to solid plug will experience three resistances: (i) due to thermal conductivity of the liquid layer, (ii) at the interface and (iii) due to thermal conductivity of solid layer. An important non-dimensional number which governs heat transfer during the phase change at the interface, is the Stefan number. It is defined as follows :

$$\text{Stefan No (Ste)} = \frac{\text{sensible heat}}{\text{Latent heat}} = \frac{C_p \Delta T}{L} = \frac{C_p (T - Tm)}{L}$$

where, Latent heat is the change in enthalpy during the phase change, C_p is the specific heat capacity (J/kgK) of the material. Since the Stefan number is a ratio of sensible heat(energy absorbed in the solid) to latent heat(absorbed at the interface), it must qualify as the resistance in terms of energy exchange offered the interface of the phase change medium. If Stefan numbers are low (< 0.2) [8], then enthalpy change at the interface is significantly higher than the heat propagated through the medium. Hence it will require longer time for the substance to melt.

The thermal properties of water and fuel salt are given in table (2.1). The temperature

Sr No	Properties	Water (@ 329.5 K)	Salt(@ 973K)
1	Density $\rho(kg/m^3)$	985.65	4124.87
2	Thermal Conductivity $\lambda(Wm/K)$	0.6458	1.0049
3	Heat Capacity $C_p(J/KgK)$	4186.025	1.049
4	thermal diffusivity $\alpha(m^2/s)$	$1.565 * 10^{-7}$	$1.536 * 10^{-7}$
5	latent heat of Fusion L (J/kg)	$3.34 * 10^5$	$1.71 * 10^5$

Table 2.1: Thermal properties of water and fuel salt

The properties of fuel and fertile salt are measured for the salt 78% LiF4- 22% ThF4 (ISTC Project No.3749)[16]
The latent heat of fusion for the salt is calculated by weighted average (based on molar mass percentage) of individual components LiF4 and ThF4 [4]
The properties of water are interpolated from the reference temperature data points provided in[11]

of ice , for further discussion, is assumed to be $-20°$C. In order to scale the temperature of water Stefan number of salt and water are equated:

$$\text{Ste}_{water} = \text{Ste}_{salt}$$

$$\Delta T_w = \frac{L_w}{L_s} \frac{C_{p_s}}{C_{p_w}} \Delta T_s = 56.5$$

Chapter 3

Analytical Solution

3.1 A simplified Model

The process described from equations (2.1) to (2.5) represent a time dependant boundary condition. Further one of the boundary, the interface position $\delta(t)$, changes with time itself. These conditions are to be further simplified to derive an analytical solution. It is also represent in fig(3.1)

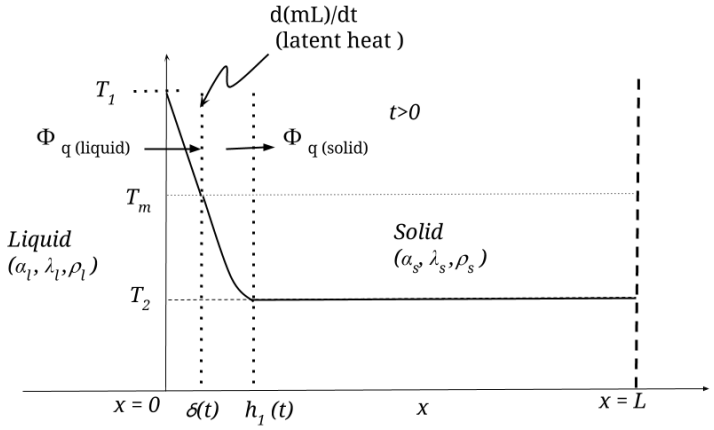

Figure 3.1: Further simplification of the model incorporates assumption of constant temperature of the liquid.

The following assumptions are made to solve the analytical solution:

i The properties of the solid phase and liquid phase are different, but they don't change with the operating temperature range for the freeze plug and over the time of melting.

ii Heat is transferred only in x-direction via conduction. Conduction is indeed the dominant heat transport mechanism. The assumption also implies that the density changes due to phase change is neglected. For water, phase change will cause volume compression $\rho_w > \rho_i$, but this should be negligible compared to the water already present in the initial liquid layer above the plug (neglecting the convection effects).

iii The temperature of the reactor is constant during the melting time of the freeze plug. This is the most unrealistic assumption of the problem. This also means that now the source of heat is simply the temperature difference between liquid in the reactor and solid plug.

iv The melting point of the solid is considered to be constant. Based on the phase change understanding, this is a valid assumption for water/ice system but not for the fuel salt.

v Solid plug is a semi-infinite medium with $x \to \infty, T_{(x,t)} = T_2$. This is a conservative approach, compared to the actual physical process, applied to derive the analytical solution. This temperature would be expected to be higher than T_2, since the solid is of finite size and the penetration of heat into the solid plug would result in an increase of temperature at x=l.

The equation governing this transport mechanism is given by equation (3.1) and (3.2)

$$\frac{\partial T(x,t)}{\partial t} = \alpha_s \frac{\partial^2 T(x,t)}{\partial x^2}\bigg|_{solid} \tag{3.1}$$

$$\frac{\partial T(x,t)}{\partial t} = \alpha_l \frac{\partial^2 T(x,t)}{\partial x^2}\bigg|_{liquid} \tag{3.2}$$

The boundary conditions for the this equation can be summed as below:
For liquid phase:

$$T(x,0) = T_1 \tag{3.3}$$

For solid phase:

$$\lim_{x\to\infty} T(x,t) = T_2 \tag{3.4}$$

Common boundary conditions for liquid-solid interface ($x = \delta$) is:

$$T_s = T_l = T_m \tag{3.5}$$

The energy balance at this interface:

$$\lambda_l \frac{\partial T(x,t)_s}{\partial x}\bigg|_{x=\delta} + L\rho_s \frac{d\delta}{dt} = \lambda_s \frac{\partial T(x,t)_l}{\partial x}\bigg|_{x=\delta} \tag{3.6}$$

Solving, the liquid phase temperature can derived to be :

$$T_{liquid}(x,t) = T_1 + \frac{(T_m - T_1)\,\mathrm{erf}\left(\frac{x}{2\sqrt{\alpha_l t}}\right)}{\mathrm{erf}(p)} \tag{3.7}$$

in eq. (3.7), erf is the error function which is defined as:

$$\mathrm{erf}(z) = \frac{2}{\sqrt{\pi}} \int_0^z e^{-x^2} dx$$

The equation for the solid phase is,

$$T(x,t)_{solid} = T_2 - (T_2 - T_m)\frac{\mathrm{erfc}\left(\frac{x}{2\sqrt{\alpha_s t}}\right)}{\mathrm{erfc}\left(p\sqrt{\frac{\alpha_l}{\alpha_s}}\right)} \tag{3.8}$$

where erfc is the complementary error function. This is defined as:

$$\text{erfc}(z) = 1 - \text{erf}(z)$$

The position of interface as a function of time is given by :

$$\delta = 2p\sqrt{\alpha_l t} \tag{3.9}$$

where p is a constant, independent of time. It is defined by the following transcendental equation:

$$\lambda_l \left(\frac{T_m - T_1}{\sqrt{\pi \alpha_l}} \frac{\exp(-p^2)}{\text{erf}(p)} \right) + L\rho_s(p\sqrt{\alpha_l}) = \lambda_s \left(\frac{T_2 - T_m}{\sqrt{\pi \alpha_s}} \frac{\exp\left(-p^2 \frac{\alpha_l}{\alpha_s}\right)}{\text{erfc}\left(p\sqrt{\frac{\alpha_l}{\alpha_s}}\right)} \right) \tag{3.10}$$

As seen from the equation, the thickness of ice melted depends on the constant p and thermal diffusivity of the source(liquid in this case). Also p is further dependant on thermal properties of solid and liquid, as well as the latent heat of fusion. The derivation of equation (3.10) can be found in A.1

In order to develop further understanding, the previous equations can also be expressed in terms of non dimensional parameters. The various non dimensional parameters involved in the process are :

$$\text{Stefan No (Ste)} = \frac{\text{sensible heat}}{\text{Latent heat}} = \frac{C_p \Delta T}{L}$$

$$\text{Fourier No (Fo)} = \frac{\text{process time}}{\text{effective time for heat conduction}} = \frac{\alpha t}{l^2}$$

$$\sigma(\text{dimensionless melt thickness}) = \frac{\delta}{l}$$

Stefan number is specifically for phase change problems whereas Fourier Number (Fo) is a common parameter to study transient heat conduction problems. The significance of Stefan No is already explained in section(2.1). Fo is the ratio of square of two length scales, thermal length (the length up to to which temperature changes are noticeable) to the actual dimensions of the body.

Re-expressing the required equations [3.7, 3.8, 3.9] in non dimensional form , we have:

$$\theta_l = \frac{T_{(x,t)} - T_1}{T_m - T_1} = \frac{\text{erf}\left(\frac{1}{2\sqrt{Fo_l}}\right)}{\text{erf}(p)}$$

$$\theta_s = \frac{T_{(x,t)} - T_2}{T_m - T_2} = \frac{\text{erfc}\left(\frac{1}{2\sqrt{Fo_s}}\right)}{\text{erfc}\left(p\sqrt{\frac{\alpha_l}{\alpha_s}}\right)}$$

$$-Ste_l \frac{\rho_l}{\rho_s} \frac{\exp(-p^2)}{\text{erf}(p)} = -p\sqrt{\pi} + Ste_s \sqrt{\frac{\alpha_s}{\alpha_l}} \frac{\exp\left(-p^2 \frac{\alpha_l}{\alpha_s}\right)}{\text{erfc}\left(p\sqrt{\frac{\alpha_l}{\alpha_s}}\right)}$$

3.2 Reference Experiment

Various experiments were studied from literature and the paper published by Ramazan Kahraman et al. [9] was found to be most effective to establish a correlation with the model described earlier. In this paper, both numerical simulation and experiments are performed for two-dimensional ice melting configuration in a rectangular enclosure. Initially water is frozen in a box (0.2 x 0.2 x 0.005 m^3) to -30 °C. It is then placed in an ice/water bath as shown in figure. Although there is heat loss, in the paper this is mathematically modelled as constant flux conditions at the boundaries at which ice bath and frozen ice are in contact with each other. The top surface of ice is placed in thermal contact with a copper box with hot water at 70 °C. This is maintained at constant temperature with the help of circulating reservoir.

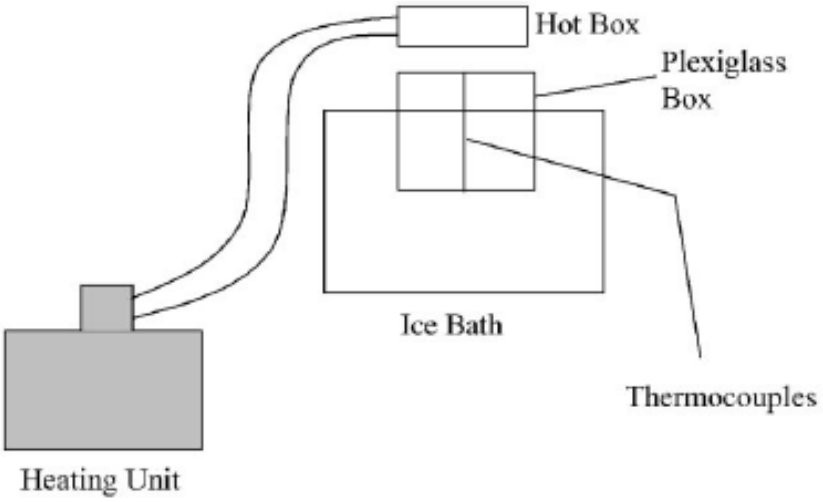

Figure 3.2: Setup of the experiment performed by Ramazan to validate the numerical model presented in [9].

The results obtained from these experiments and numerical simulation will be compared with the results obtained from the analytical model.

3.3 Sensitivity Analysis

Till now, the physical phenomena has been described and it has been translated into a mathematical model. The physical parameters of importance are related to output through mathematical equations. Sensitivity analysis enables to describe the change in output parameter with respect to change in the input parameter [12]. In this case, one of the output is the position of the interface which is described by

$$\delta = 2p\sqrt{\alpha_l t}$$

Further dependence of p on other parameters is expressed as :

$$\lambda_l \frac{T_m - T_1}{\sqrt{\pi\alpha_l}} \frac{\exp(-p^2)}{\text{erf}(p)} + L\rho_s(p\sqrt{\alpha_l}) = \lambda_s \frac{T_2 - T_m}{\sqrt{\pi\alpha_s}} \frac{\exp\left(-p^2\frac{\alpha_l}{\alpha_s}\right)}{\text{erfc}\left(p\sqrt{\frac{\alpha_l}{\alpha_s}}\right)}$$

The only independent parameter in the physical model is time. Temperature and the interface position δ is dependent variable. They depend on the material parameters, such as $\alpha, \lambda, \rho, C_p, L$ etc. The dependent variable of interest here is the position of interface, since total time to melt the plug and the final flow of liquid salt from the core to the drain tank is to be calculated. Since the physical model is translated from material of LiF4-ThF4 to water/ice, it is important to understand the change in interface position with respect to changes in material properties.

The parameters chosen for sensitivity analysis are initial temperature of ice (T_2), thermal conductivity of water (λ_w), and Latent Heat(L). Initial temperature for the actual plug design and water/ice model are unknown, hence it would be important to study sensitivity of the interface position with respect to these parameter. Thermal conductivity is chosen because δ is directly dependent on λ and heat transport is dominated by conduction. Finally latent heat is evaluated because its theoretical value for salt was approximated to calculate the Stefan number. It also represent the energy required for the phase change.

The equation of properties of liquid $LiF - ThF_4$ as function of temperature are given in [16]. These are described as below:

$$\rho_{salt} = 4.094 - 8.82 \cdot 10^{-4} \cdot (T) - 1008)$$

ρ is g/cm^3

$$\lambda_{salt} = 0.928 + 8.397 \cdot 10^{-5} \cdot T$$

λ is W/mK

$$C_{p_{salt}} = (-1.111 + 0.00278 \cdot T) \cdot 10^3$$

C_p is in J/kgK. Here all the temperature T are substituted in kelvin. The temperature dependence of properties of molten salt and water is plotted below 3.3 and 3.4. The temperature range for salt is between 798 K to 1073 K while for water the temperature range between 273 K to 373K. The properties of salt and water exhibit similarity in nature i.e thermal conductivity increases with temperature while the density decreases with increase in temperature. Based on this it possible to say that sensitivity behaviour with respect to these parameter could be approximated.

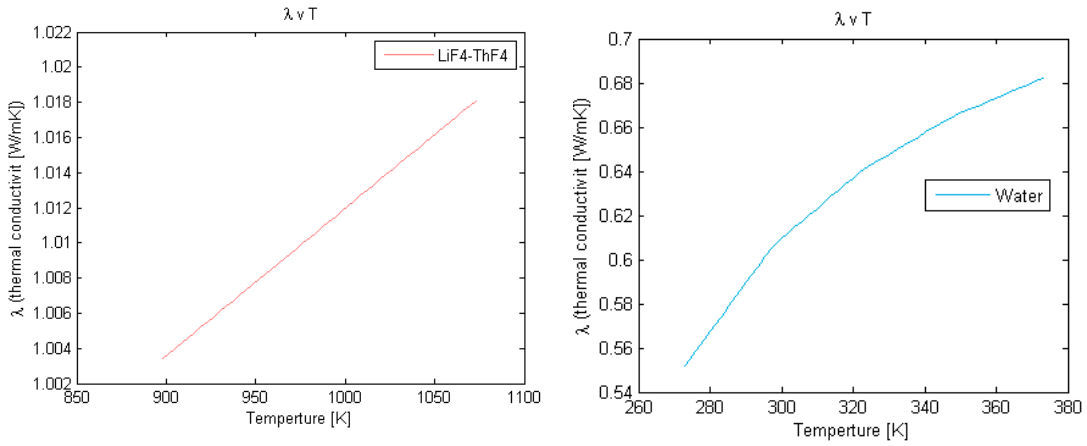

(a) thermal conductivity of molten salt as a function of temperature

(b) thermal conductivity of water as a function of temperature

Figure 3.3: Comparative study of thermal conductivity of water and salt for respective temperature range.

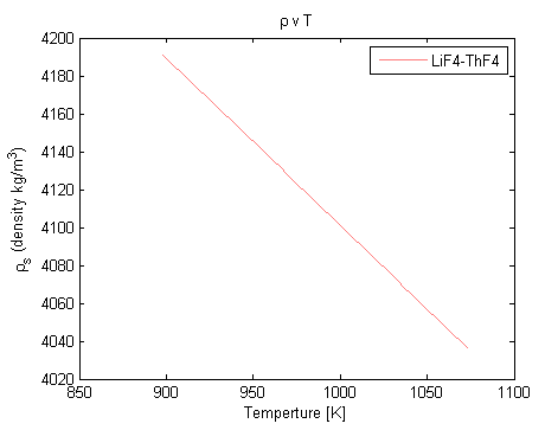

(a) thermal conductivity of molten salt as a function of temperature

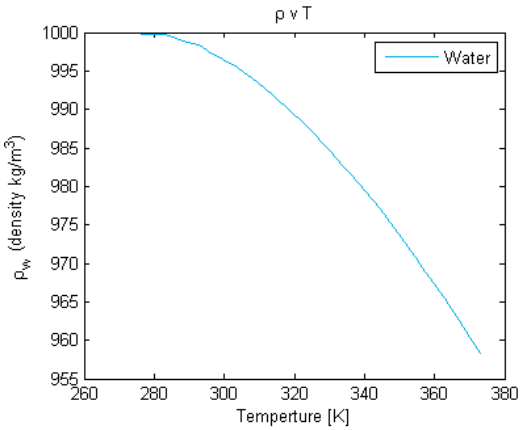

(b) thermal conductivity of water as a function of temperature

Figure 3.4: Comparative study of density of water and salt for respective temperature range.

Approach for sensitivity analysis is as follows:

i Change the required parameter over a range of values. For example λ is varied over the range of 0.2 to 1.5 W/mK

ii Calculate the constant p due change in parameter and determine the new interface position.

iii Based on this $\Delta\delta/\Delta\lambda$ is calculated which represent the sensitivity of δ with change in λ. This slope is then plotted versus λ itself. This process is repeated for other parameters.

Chapter 4

Results

4.1 Results and Discussion

In order to solve the equation for p, a Matlab code (A.2) is used. The thermal properties of ice are calculated according to the equation given in [6] while values for thermal properties of water are extrapolated from the data given in [11]. In figure (4.2a) the ratio of δ/l is plotted on the y-axis and simulation time is plotted on x-axis. In the figure (4.2b), reference experiment graph of melting thickness vs time is plotted. For all the matlab calculations, a finite length of 10 cms of salt is assumed. The temperature values used in the analytical model $T_{water} = 56.5°\text{C}$ whereas in the experiment it was 70°C as for T_{ice}, in the analytical model it is $-20°\text{C}$ whereas for experiment it is $-30°\text{C}$. Hence, for the analytical solution, the temperature values are modified to experiment values to have exact comparison.

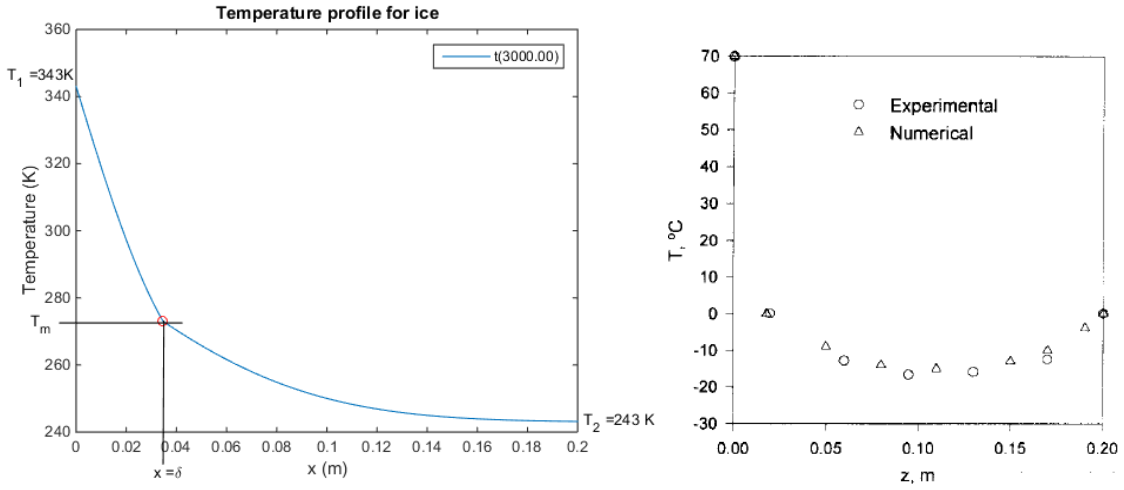

(a) Analytical result

(b) Reference result from [9]

Figure 4.1: Comparative study of temperature distribution of ice with respect to position for different methods. Fig.(a)Simulation result for 1D analytical model computed from Matlab Fig.(b) Comparison of numerical model at the midway along the width (t= 3000 secs) of the melting ice block from the reference paper.

Temperature Distribution: Figure(4.1a) shows the temperature distribution in the ice obtained from the analytical solution while figure(4.1b) shows the temperature distribution in the ice obtained from the experiment results. Both plots correspond to t=3000 secs. The temperature distribution profiles obtained from analytical and experimental results is indeed similar. Two distinct gradients can be seen in the graph due to variation in conductivities of the water and ice. Both analytical and experimental results show steep

temperature gradient for water layer. Also, the interface position is indeed identified by the T=Tm. Since experiment model allows heat loss at x=0.2 end, the temperature at this end rises whereas for analytical result ice is assumed to be semi infinite solid layer. This also facilitates faster melting times in experimental model when compared to analytical.

In order to obtain a better correlation with above experimental results, one of the boundary condition: $T_{(x,t)} = T_2, x \to \infty$ has to replaced with a new boundary condition, at x=L for a finite plug. For the plug, it is expressed in eq. 2.4. The solution for this type of boundary condition can no longer be solved analytically. Temperature profile can be assumed based on recommendations by [1] and [13] and solved approximately by integral heat balance method. This temperature profile is a polynomial expression. Since the error function provides good correlation with experimental results, it could be also possible to obtain a polynomial fit through Taylor series expansion of the error function given below:

$$\text{erf}(z) = \frac{2}{\sqrt{\pi}}\left[z - \frac{z^3}{3} + \frac{z^5}{10}.....\right]$$

Hence, a polynomial approximation of temperature in solid would be:

$$T_{solid}(x,t) = a(t) + b(t)\frac{2}{\sqrt{\pi}}(x - \delta(t)) + c(t)\frac{2(x-\delta(t))^3}{3\sqrt{\pi}} \tag{4.1}$$

where l is the length of the plug. $a(t)$, $b(t)$, $c(t)$ are the coefficients of polynomial which should be found using the boundary conditions defined for the problem.

Melting Thickness: Figure (4.2a) shows the melting thickness vs time for analytical model, while (4.2b) shows the results from experimental and numerical results. One of the main drawback of neglecting an external heat source is evident in fig(4.2a). Melting times are much higher than design requirement of 11 minutes.

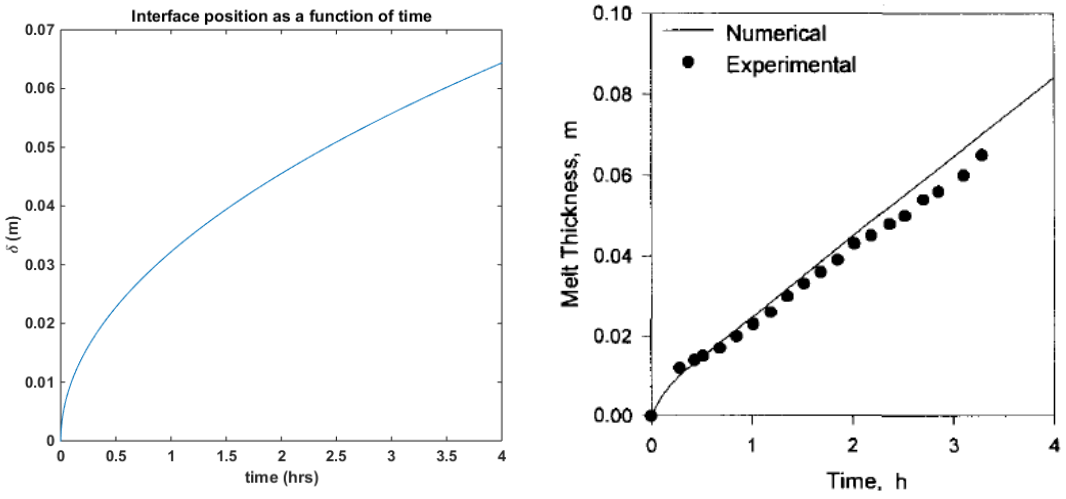

(a) Analytical result

(b) Reference result from [9]

Figure 4.2: Comparative study of melting thickness of ice with respect to time for different methods. Figure(a) shows the simulation result for 1D analytical model computed from matlab. Figure(b) shows the comparison of numerical model at the midway along the width (x=10 cm) of the melting ice block from the reference paper.

As per analytical derivation, δ is $F(\sqrt{t})$ and hence the velocity of the interface is $F(1/\sqrt{t})$. This implies that as time increase, the velocity of the interface decreases. As explained in the section (2.1.2), the heat transfer experiences three different resistances.

Resistance to conductive heat transfer can be calculated as :

$$R_{heat} = \frac{l}{\lambda A}$$

where l is the length dimension and A is the area of cross section.

$$R_w = \frac{l(t)}{\lambda_w A}$$

In case of water/ice system $\lambda_w = \lambda_i/3$, hence the resistance R, $F(1/\lambda)$, offered by water layer is 3 times more than ice. As time increases, the water layer thickness increases, the resistance offered by water layer increases and hence the melting process becomes slower as time progress. This is also significant because only conduction is considered as primary mechanism of heat transfer.

Further, the nature of the curve in analytical model is also quite different from the experimental results. The melting thickness predicted by analytical model after t=1 hr is 0.0322m while in the experiment it is less than 0.03m. Moreover, the melting thickness at the end of 4 hrs as predicted by analytical solution is 0.0628m whereas from the experimental results it is 0.08m. It seems that if two curves were to be plotted together, experimental time of melting would be lower initially and then be higher than analytical model. Thus additional natural heat transfer mechanism must be present in the experimental setup which is the onset of natural convection due to temperature variation in the liquid layer and volumetric compression caused by melting of ice. Clearly, in absence of external heat source, conduction is not the only dominant phenomenon. Insulated boundary condition also have effect on heat transfer inside the ice, hence the temperature distribution and subsequently the melting times.

4.1.1 Sensitivity Analysis

Thermal Conductivity: In the figure 4.3, a two y-axis graph is plotted.The x-axis represents the range of λ, while the right y-axis represents the interface position and the left y axis represent the slope of this curve. As discussed, this slope represent the sensitivity of δ with respect to λ. As seen from the graph, interface position increases with the thermal conductivity. This is evident from the eq(3.9) since interface position directly proportional to $\sqrt{\lambda}$. The sensitivity of this change is higher for lower values of λ and it decreases as λ increases. Thermal conductivities can be conceptualised same as electrical conductivities but for heat transport. Hence a material with low thermal conductivity (for example water λ_{water}= 0.65 W/mK) would be an thermal insulator while a material with high thermal conductivity would a conductor of heat.(for ex ice λ_{ice}= 1.8973 W/mK). Since a conductor would allow easier transport of heat, the sensitivity of interface position is quite low for high values of λ. Also, the assumption of assuming λ_w as independent of temperature still provides good approximation. λ_w varies from 0.5 to 0.682 over a temperature range of 273K to 373K and in this region change in δ is less than 1%. Furthermore, the $\lambda_{salt} > 1$ W/mK hence plug of salt would expect to melt faster than that of ice.

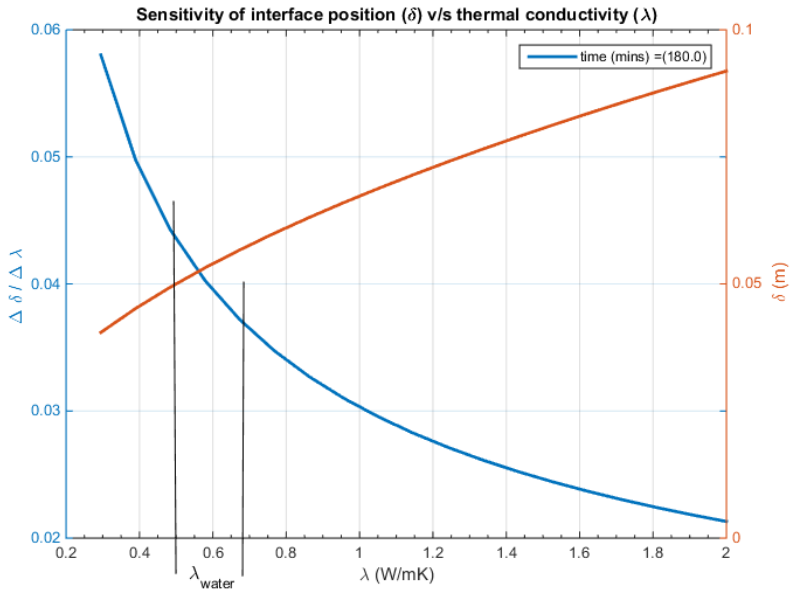

Figure 4.3: Sensitivity analysis for thermal conductivity (λ)

Latent heat of Fusion: Similarly, figure 4.4 shows the sensitivity of latent heat with interface position on a two axis graph. Due to the assumption of constant temperature difference between the liquid and the solid plug, the amount of energy available for melting via conduction is constant. As the latent heat of fusion increases, the interface position becomes lower as more energy is required to melt the plug. This also implies that $\Delta\delta$ is negative. It also implies that, as observed in the graph, the sensitivity decreases for higher values of L. The approximated value of L_{salt} is equal to 1.71 x 10^5 J/kg which is much lower than that of ice. Based on δ vs L curve, this would imply that the plug would melt completely in 3 hrs for a length of 8 cm. Also, the sensitivity of interface position is quite high in this region, hence it would be required to accurately determine the latent heat for salt.

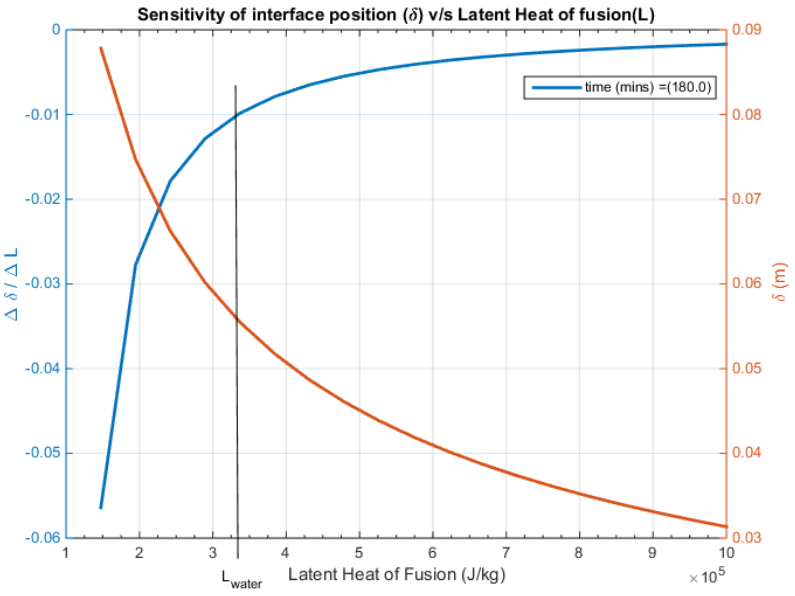

Figure 4.4: Sensitivity analysis for Latent Heat of Fusion (L)

Initial Temperature of the plug: The temperature changes of ice for the calculation of sensitivity varies from $-3°C$ to $-20°C$. The time of simulation is 3000 seconds. Following the same procedure as for other parameters, figure (4.5a) shows the sensitivity plot for variation in initial temperature of ice (T_2). Although the graphs show increasing trend with lowering T_2, the changes are really insignificant. Mathematically, the dependence of δ is implicitly defined with T_2 through parameter p. The variation in this parameter p is very low because of the variation in T_2 which is reflected in δ.

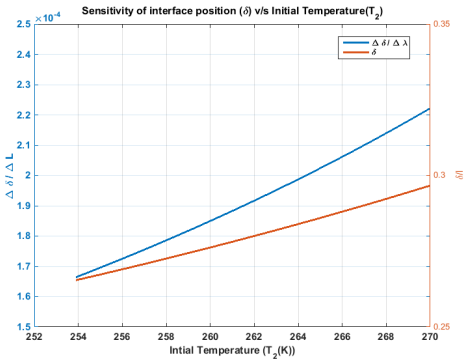

(a) Sensitivity analysis for Initial Temperature of ice.

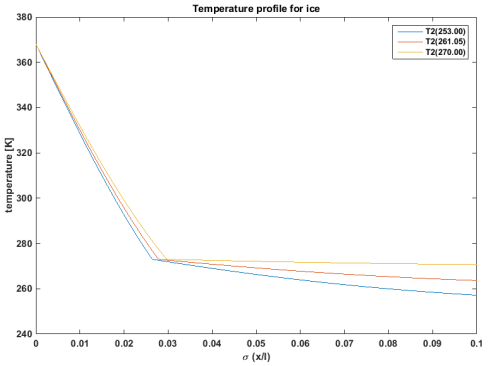

(b) Temperature profiles for ice from the matlab code.

Figure 4.5: Figure(a) shows the effect of variation of initial temperature of ice and δ while in figure(b) temperature distribution inside ice is plotted vs σ

An another interesting result from variation of T_2 is that, there is no significant changes in the temperature distribution as shown in fig(4.5b). The changes in the temperature of ice influence the temperature of water only by virtue of shift in interface position. This is also a confirmation of sensitivity analysis made above. One of the possible explanation could be due low Stefan number on of ice. This implies that most of the energy is absorbed as latent heat for ice.

$$Ste_{ice} = \frac{C_{p_i}\Delta T}{L} = \frac{1.876 \cdot (273 - 253)}{33400} = 0.1553$$

Another possible explanation could be that it is a limitation of 1D semi infinite pure conduction model. It is unable to incorporate other form of heat transfer from liquid to the plug via convection, which will eventually influence the temperature distribution and interface position for the plug. In [5], a detailed experiment is performed for a different phase change material and different geometry of plug, with varying initial temperature of liquid to study the effect of convection. A simple equation describing energy balance at the interface position is derived in both [5] and [9]:

$$q_l = -\lambda_s A \frac{\partial T(x,t)}{\partial x}\bigg|_{x=\delta} + L\rho_s A \frac{d\delta}{dt}$$

where q_l is the heat flux from the liquid side. A possible approximation suggested in [5], is dropping the heat flux term of the solid if the temperature of solid is close to T_m. This result also resembles the boundary condition provided in eq: (2.5), as a part of first model in which q_l is replaced by $P_{decay}(t)$. Indeed, the assumptions made to further simply the original model, in order to derive a mathematical expression, has caused deviation from experimental results.

Chapter 5

Conclusions and Recommendations

5.1 Conclusions

In conclusion, based on the simple 1D analytical model, the required melting time for a plug of 10 cms was beyond the requirement of 10 min. In analytical model the plug, was infinite but in reality it has to be of finite length. Primary requirement to model this would be to replace the condition: $T_{(x,t)} = T_2, x \to \infty$ with a new boundary condition given by eq:(2.4) at x=L for the plug. On comparison of the analytical model with an reference experiment, the temperature distribution were in agreement and similar in nature. But the results of interface position in analytical model is a $F(\sqrt{t})$ while in experimental result they are linear in nature. This is attributed to the increase in the heat resistance from the water layer over time. As discussed in 3.3, results from sensitivity analysis can be extrapolated to molten $LiF - ThF_4$ properties for the 1D conduction model . Based on this, it would be expected that the freeze plug made of solidified $LiF - ThF_4$ has the potential to melt faster due to higher thermal conductivity and lower latent heat of fusion of the molten salt. Further sensitivity analysis show very little dependence of δ on the initial temperature of ice (T_2). Change in T_2 also does not show a significant influence on the temperature distribution. This is attributed to very low Stefan number of ice and neglecting effects of convection.

5.2 Recommendations

The phase change process of freeze plug is complex phenomena dependant on many different parameters such as:

- how $LiF - ThF_4$ undergoes phase change ;
- thermal properties of liquid and solid $LiF - ThF_4$ system ;
- different assumptions and subsequent boundary conditions to model this phenomena

Based on this following recommendations are made

- **Materials:** Since the properties of the solid $LiF - ThF_4$ are still unknown, the scope for using other materials for freeze plug, should be studied. Ice is modelled as freeze plug in this report, since its properties and behaviour with $LiF - ThF_4$ is known. If it were to be actually used a plug, then due to the large temperature difference between the reactor core ($T_1 = 973$) and the melting temperature of ice ($T_m = 273$),

it would require enormous cooling power, during normal operating conditions, in order to be maintained at T_m. Also, other molten salts such as LiF, BeF_2 or NaF could be consider for the freeze plug application.

- **Experiments:** The experiments from reference literature [9] and [5] utilized to establish a correlation, are different from the actual reactor core- freeze plug system. They do not have an external heat source to melt the phase change material which could influence the dominant mechanism of heat transfer. Also, the experiments performed to validate the original freeze plug design [3], involved uniform heating of the plug which allows faster melting times. Hence, an experiment should be performed to be mimic the actual behaviour of this system.

- **Mathematical Model:** The main difficulty in solving the melting problem analytically is incorporating time dependent boundary conditions. Based on correlation, in eq: (4.1), an approximate temperature profile in polynomial form is provided. It should be further evaluated by solving using the boundary conditions described from eq:(2.2 to 2.5). This could be then validated with either new experiments or experiment performed in [3].

Acknowledgements

Firstly, I would like to thank Prof.Dr.ir.Jan Leen Kloosterman for giving me the opportunity to work on this project. I enjoyed working on it with you. Secondly, I would like to thank Dr. ir M. Rohde , Matteo Gamarino, Sagar Harinarayan and Nisarg Gandhi with whom I had many discussions that influenced my understanding of the project and they also provided valuable feedbacks for my report.

Appendix A

Appendix

A.1 Analytical Solution

The equation governing this transport is given by equation [A.1] and [A.2]

$$\frac{\partial T}{\partial t} = \alpha_s \frac{\partial^2 T}{\partial x^2}\bigg|_{solid} \tag{A.1}$$

$$\frac{\partial T}{\partial t} = \alpha_l \frac{\partial^2 T}{\partial x^2}\bigg|_{liquid} \tag{A.2}$$

where,

$$\alpha_s = \frac{\lambda_s}{\rho_s C_p}$$

$$\alpha_l = \frac{\lambda_l}{\rho_l C_p}$$

The boundary conditions for the this equation can be summed as below:
For liquid phase:

$$T_{(x,0)} = T_1 \tag{A.3}$$

For solid phase:

$$\text{As}, x \to \infty, T_{(x,t)} = T_2 \tag{A.4}$$

The implies that temperature much further away from the front is T_2. This temperature would be expected to be higher than T_2, since the solid is of finite size and the penetration of heat would result in increase in temperature at the far end.

Common boundary conditions ($x = \delta$):

$$T_s = T_l = T_m \tag{A.5}$$

This implies that the interface temperature of the boundary is equal to the melting temperature.

Now consider the energy balance at this interface:

$$\phi_{in} - \phi_{out} + \text{Production/Destruction} = 0$$

$$\left(-\lambda_l A \frac{\partial T}{\partial x}\bigg|_{x=\delta}\right) - \left(-\lambda_s A \frac{\partial T}{\partial x}\bigg|_{x=\delta}\right) - \frac{L dm_s}{dt} = 0$$

where,

A : the cross section area for heat transfer

L : the latent heat of fusion

λ : thermal heat conductivity

The second term determines the amount of heat utilized in melting of the solid phase. The negative sign for this, signify decrease in the mass of solid with increasing time. Substituting,

$$\frac{Ldm_s}{dt} = L\frac{d(\rho_s V)}{dt} = L\frac{d(\rho_s A\delta)}{dt} = L\rho_s A\frac{d\delta}{dt}$$

and cancelling out A and minus sign, we get

$$\lambda_l \frac{\partial T_l}{\partial x}\bigg|_{x=\delta} + L\rho_s \frac{d\delta}{dt} = \lambda_s \frac{\partial T_s}{\partial x}\bigg|_{x=\delta} \tag{A.6}$$

The procedure to solve the equation with these boundary conditions is followed from the textbooks [14] and [10]. One can use Laplace transformation, to solve the system of equation, as follow:

$$\mathscr{L}\left(\frac{\partial T}{\partial t}\right) = -T_{(x,0)} + s\bar{T}_{(x,s)}$$

$$\mathscr{L}\left(\frac{\partial^2 T}{\partial x^2}\right) = \frac{\partial^2 \bar{T}}{\partial x^2}$$

Hence the equation after transformation becomes,

$$-T_{(x,0)} + s\bar{T}_{(x,s)} = \alpha\frac{\partial^2 \bar{T}}{\partial x^2}$$

This can solved with the substitution :

$$-T_{(x,0)} + s\bar{T}_{(x,s)} = u$$

then,

$$\frac{\partial^2 \bar{T}}{\partial x^2} = u''$$

$$u'' = \frac{s}{\alpha}u$$

The solution to this equation is given by:

$$u = A\exp\left(\frac{s}{\alpha}x\right) + B\exp\left(-\frac{s}{\alpha}x\right)$$

A and B are constants of integration. Since the solution is finite even if $x \to \infty$ A=0. Hence equation reduces to

$$u = B\exp\left(-\frac{s}{\alpha}x\right)$$

Re-substituting value of u, we get

$$-T_{(x,0)} + s\bar{T}_{(x,s)} = B\exp\left(-\frac{s}{\alpha}x\right)$$

Dividing the equation by s and rearranging terms,

$$\bar{T}_{(x,s)} = \frac{T_{(x,0)}}{s} + \frac{B\exp\left(-\frac{s}{\alpha}x\right)}{s}$$

transforming this equation back using Laplace transformation tables , we get

$$T_{(x,t)} = T_{(x,0)} + B\,\mathrm{erf}\left(\frac{x}{2\sqrt{\alpha t}}\right)$$

where erf is the error function. the error function is defined as:

$$\mathrm{erf}(z) = \frac{2}{\sqrt{\pi}}\int_0^z e^{-x^2}dx$$

For liquid phase, solving with boundary conditions A.5, we have,

$$T_{(x,0)} = T_1$$

and using condition A.6 we have,

$$T_m = T_1 + B\,\mathrm{erf}\left(\frac{\delta}{2\sqrt{\alpha_l t}}\right)$$

The left hand side of the equation is constant , while the right hand side of the equation is function of time. To satisfy this condition , $\delta \propto \sqrt{t}$ must be satisfied. Introducing a parameter p (constant) such that,

$$p \equiv \frac{\delta}{2\sqrt{\alpha_l t}}$$

therefore, the value of B is given by,

$$B = \frac{T_m - T_1}{\mathrm{erf}(p)}$$

So, the solution for liquid phase becomes,

$$T_{(x,t)}\big|_{liquid} = T_1 + \frac{(T_m - T_1)\,\mathrm{erf}\left(\frac{x}{2\sqrt{\alpha_l t}}\right)}{\mathrm{erf}(p)} \tag{A.7}$$

we can rewrite the solution for solid phase:

$$T_{(x,t)} = C + D\,\mathrm{erf}\left(\frac{x}{2\sqrt{\alpha_s t}}\right)$$

Similarly for solid phase the boundary conditions are governed by A.4 and A.5 , we get

$$C + D = T_2$$
$$T_m = C + D\,\mathrm{erf}\left(\frac{\delta}{2\sqrt{\alpha_s t}}\right)$$

Subtraction these conditions to eliminate C,

$$T_2 - T_m = D\,\mathrm{erfc}\left(\frac{\delta}{2\sqrt{\alpha_s t}}\right)$$

$$D = \frac{T_2 - T_m}{\mathrm{erfc}\left(\frac{\delta}{2\sqrt{\alpha_s t}}\right)}$$

Substituting the value of δ from the previous reasoning, we get

$$D = \frac{T_2 - T_m}{\mathrm{erfc}\left(p\sqrt{\frac{\alpha_l}{\alpha_s}}\right)}$$

$$C = T_2 - \frac{T_2 - T_m}{\operatorname{erfc}\left(p\sqrt{\frac{\alpha_l}{\alpha_s}}\right)}$$

So, the solution for solid phase becomes,

$$T_{(x,t)}\big|_{solid} = T_2 - \frac{T_2 - T_m}{\operatorname{erfc}\left(p\sqrt{\frac{\alpha_l}{\alpha_s}}\right)} + \frac{(T_2 - T_m)\operatorname{erf}\left(\frac{x}{2\sqrt{\alpha_s t}}\right)}{\operatorname{erfc}\left(p\sqrt{\frac{\alpha_l}{\alpha_s}}\right)} \tag{A.8}$$

The constants in the temperature equation of solid phase and liquid phase do depend on properties of the liquid and solid respectively.

The only unknown in both the temperature equation A.7 and A.8 is p. It can be found using the final interface boundary condition:

$$\lambda_l \frac{\partial T_l}{\partial x}\bigg|_{x=\delta} + L\rho_s \frac{d\delta}{dt} = \lambda_s \frac{\partial T_s}{\partial x}\bigg|_{x=\delta}$$

Now,

$$\frac{\partial T_l}{\partial x}\bigg|_{x=\delta} = \frac{T_m - T_1}{\operatorname{erf}(p)} \frac{d\left(\operatorname{erf}\frac{x}{2\sqrt{\alpha_l t}}\right)}{dx}$$

by definition,

$$\frac{d(\operatorname{erf}(x))}{dx} = \frac{2}{\sqrt{\pi}} \exp(-x^2)dx$$

$$= \frac{2}{\sqrt{\pi}} \exp(-\frac{\delta^2}{4\alpha_l t}).\frac{1}{2\sqrt{\alpha_l t}}$$

Substituting value of δ , we have

$$= \frac{1}{\sqrt{\pi\alpha_l t}} \exp(-p^2)$$

thus,

$$\frac{\partial T_l}{\partial x}\bigg|_{x=\delta} = \frac{T_m - T_1}{\operatorname{erf}(p)} \frac{1}{\sqrt{\pi\alpha_l t}} \exp(-p^2)$$

similarly ,

$$\frac{\partial T_s}{\partial x}\bigg|_{x=\delta} = \frac{T_2 - T_m}{\operatorname{erfc}\left(p\sqrt{\frac{\alpha_l}{\alpha_s}}\right)} \frac{1}{\sqrt{\pi\alpha_s t}} \exp\left(-p^2\frac{\alpha_l}{\alpha_s}\right)$$

Also,

$$\frac{d\delta}{dt} = \frac{d(2p\sqrt{\alpha_l t})}{dt} = p\sqrt{\frac{\alpha_l}{t}}$$

Substituting all the values , and cancelling $\sqrt{t}$ we have a transcendental equation for the constant p :

$$\lambda_l \left(\frac{T_m - T_1}{\sqrt{\pi\alpha_l}} \frac{\exp(-p^2)}{\operatorname{erf}(p)}\right) + L\rho_s(p\sqrt{\alpha_l}) = \lambda_s \left(\frac{T_2 - T_m}{\sqrt{\pi\alpha_s}} \frac{\exp\left(-p^2\frac{\alpha_l}{\alpha_s}\right)}{\operatorname{erfc}\left(p\sqrt{\frac{\alpha_l}{\alpha_s}}\right)}\right) \tag{A.9}$$

In order to verify the derivation , we can substitute the conditions for same material properties $\lambda_s = \lambda_l = \lambda$; $\alpha_s = \alpha_l = \alpha$ and $\rho_s = \rho_l = \rho$. hence the equivalence of p changes to $\frac{\delta}{2\sqrt{\alpha t}}$.

Hence the equation A.7 reduces to :

$$\lambda\left(\frac{T_m - T_1}{\text{erf}(p)}\frac{\exp(-p^2)}{\sqrt{\pi\alpha}}\right) + L\rho p\sqrt{\alpha} = \lambda\left(\frac{T_2 - T_m}{\text{erfc}(p)}\frac{\exp(-p^2)}{\sqrt{\pi\alpha}}\right)$$

Multiplying throughout by $\sqrt{\pi\alpha}$, substituting α as $\frac{\lambda}{\rho C_p}$ and then cancelling lambda throughout the equation :

$$\exp(-p^2)\frac{T_m - T_1}{\text{erf}(p)} + p\sqrt{\pi}\frac{L}{C_p} = \exp(-p^2)\frac{T_2 - T_m}{\text{erfc}(p)}$$

The results are in agreement with [10, 14, 13]

A.2 Matlab Code

A.2.1 Fourier Number

```
% %
clear
clc
% Program to solve non dimensional analytical solution of the moving front pr
% ice and water as an example
%Effect of Fourier Number


l= 0.1; %Length of ice in solid
T2= -20+273; % intial temperature of ice
T1= 56.5+273;    %Liquid temperature (K)
Tm = 0+273;      %Melting point of Solid (K)

%Properties of Ice
rho_i = 917*(1- ((T2-273)*1.17*10^-4)); %density( T :celsius)
lambda_i = 1.16*(1.91-(8.66*(10^-3)*T2)+(2.97*(10^-5)*T2^2));
% thermal conductivity W/mK
Cp_i = (0.85+ (0.689*(10^-2)*T2))*10^3;
%Heat capacity of ice J/kgK
alpha_i= lambda_i/(Cp_i*rho_i);

%Properties of water
%properties of water from data companion
R_w = [999.87,999.73,998.23,995.68,992.25,988.07,983.23,977.93,971.82,965.34
T_w = 273:10:373;

l_w = [0.552,0.607,0.641,0.665,0.682];
T_l =273:25:373 ;

Cp_l= [4221,4185.0,4181.6,4187.5,4199.6,4219.3];
T_cp =273:20:373;

%properties of water;
```

```
rho_w = interp1(T_w,R_w,T1);
Cp_w = interp1(T_cp,Cp_1,T1);
lambda_w =interp1(T_l,l_w,T1);
alpha_w= lambda_w./(Cp_w.*rho_w);

L = 3.34*10^5;  %Latent heat of evaporation J/kg;

%%
% Non dimensional Numbers
Ste_s = Cp_i*( Tm-T2)/ L ; % stefan no for ice
Ste_l= Cp_w*( T1-Tm)/ L ; %stefan no for water

% calculating the constant of the soltuion
A = Ste_l*rho_w/rho_i;
B = Ste_s*sqrt(alpha_i/alpha_w);
C = sqrt(pi);
D = @(p)p*alpha_i;
E = @(p)p*alpha_w;

X1= @(p)A.*exp(-p^2)./erf(p); %Liquid
X2= @(p)C.*p; %Latent Heat
X3= @(p)B.*exp(-p^2*(alpha_w/alpha_i))./erfc(p*sqrt(alpha_w/alpha_i));
%Solid

f1=@(p)(-X1(p)+ X2(p)+ X3(p));
x0 = [0.1  10]; % initial interval
options = optimset('Display','iter'); % show iterations
[p1, fval, exitflag, output] = fzero(f1,x0,options);

t=0:1:300;
Fo1 = alpha_i*t/l^2; %fourier No

% constants for temperature profile :
Z = (T2-Tm)/erfc(p1*sqrt(alpha_w/alpha_i));
Q = (Tm-T1)/erf(p1);
d1 =length(t);
for r=1:1:d1


    delta1(r)= 100*2*p1*sqrt(alpha_w*t(r)); % thickness in cm


end
v= 100*2*p1*sqrt(alpha_w*t(r));

%Now have to define x such that x --> delta for solid
% and delta <x--> for liquid

y = linspace(v,10,d1);
x = linspace(0,v,d1);
x1(1:d1) = T1;
```

```
y1(1:d1) = T2;
t1=t(r);
for n=1:1:length(t);
q(n)=erf(x(n)/(100*2*sqrt(alpha_w*t1)));
Tw(n) = x1(n) + (Q*q(n));
thetaw(n) = (Tw(n)-T1)/(Tm-T1);     %nondimensional temperature
r(n) = (erfc(y(n)/(100*2*sqrt(alpha_i*t1))));
Ti(n) = y1(n) - (Z*r(n));
thetai(n) = (Ti(n)-T2)/(Tm-T2);     %nondimensional temperature
end
Fo_1=Fo1(n);

%%
t2=0:1:60*12;
d2=length(t2);
Fo2 = alpha_i*t2/l^2; %fourier No
for k=1:1:d2


    delta2(k)= 100*2*p1*sqrt(alpha_w*t2(k)); % thickness in cm


end
w2= delta2(k);
%Now have to define x such that x --> delta for solid
% and delta <x--> for liquid

y2 = linspace(w2,10,d2);
x2 = linspace(0,w2,d2);
u2(1:d2) = T1;
v2(1:d2) = T2;
tau2=t2(k);
for n=1:1:k;
q2(n)=erf(x2(n)/(100*2*sqrt(alpha_w*tau2)));
Tw2(n) = u2(n) + (Q*q2(n));
thetaw2(n) = (Tw2(n)-T1)/(Tm-T1);
r2(n) = (erfc(y2(n)/(100*2*sqrt(alpha_i*tau2))));
Ti2(n) = v2(n) - (Z*r2(n));
thetai2(n) = (Ti2(n)-T2)/(Tm-T2);
end
Fo_2= Fo2(k);

%%
t3=0:1:1500;
d3=length(t3);
Fo3 = alpha_i*t3/l^2; %fourier No
for j=1:1:d3


    delta3(j)= 100*2*p1*sqrt(alpha_w*t3(j)); % thickness in cm
```

```
end
w3= delta3(j);
%Now have to define x such that x --> delta for solid
% and delta <x--> for liquid

y3 = linspace(w3,10,d3);
x3 = linspace(0,w3,d3);
u3(1:d3) = T1;
v3(1:d3) = T2;
tau3= t3(j);
for n=1:1:j;
q3(n)=erf(x3(n)/(100*2*sqrt(alpha_w*tau3)));
Tw3(n) = u3(n) + (Q*q3(n));
thetaw3(n) = (Tw3(n)-T1)/(Tm-T1);
r3(n) = (erfc(y3(n)/(100*2*sqrt(alpha_i*tau3))));
Ti3(n) = v3(n) - (Z*r3(n));
thetai3(n) = (Ti3(n)-T2)/(Tm-T2);
end
Fo_3=Fo3(j);

%%

figure(2)
plot(y/(100*l),thetai,y2/(100*l),thetai2,y3/(100*l),thetai3)
xlabel('\delta (length scale)')
ylabel('\theta (Non dimensional temperature)')
title('Temperature profile for ice')
legend(sprintf('Fo_1(%0.2f)',Fo_1),sprintf('Fo_2(%0.2f)',Fo_2),
sprintf('Fo_3(%0.2f)',Fo_3))
```

A.2.2 Sensitivity Analysis of Lambda

The code has a similar structure to other parameters.

```
% %
clear
clc
% Program to solve non dimensional analytical solution of the moving
%front problem
% ice and water as an example

%%
% studying the effect of lambda on the interface position:


T1 = 56.5+273;    %Liquid temperature (K)
T2 = -20+273;     %Solid Temperature (K) from -25 to -5 C
Tm = 0+273;     %Melting point of Solid (K)
l= 0.1; %Length of ice in solid in m

%properties of water from data companion
R_w = [999.87,999.73,998.23,995.68,992.25,988.07,
```

```
983.23,977.93,971.82,965.34,958.38];
T_w = 273:10:373;

l_w = [0.552,0.607,0.641,0.665,0.682];
T_l =273:25:373 ;

Cp_l= [4221,4185.0,4181.6,4187.5,4199.6,4219.3];
T_cp =273:20:373;

%properties of water;
rho_w = interp1(T_w,R_w,T1);
Cp_w = interp1(T_cp,Cp_l,T1);
%lambda_w =interp1(T_l,l_w,T1);
%alpha_w= lambda_w./(Cp_w.*rho_w);

%Properties of Ice
rho_i = 917*(1- ((T2-273)*1.17*10^-4)); %density( T :celsius)
lambda_i = 1.16*(1.91-(8.66*(10^-3)*T2)+(2.97*(10^-5)*T2^2));
% thermal conductivity W/mK
Cp_i = (0.85+ (0.689*(10^-2)*T2))*10^3;
%Heat capacity of ice J/kgK
alpha_i= lambda_i/(Cp_i*rho_i);

L = 3.34*10^5; %Latent heat of evaporation J/kg;

t=0:10:3*60*60;

delta= ones(5,length(t));
w= ones(5,1);
x=ones(5,length(t));
y=ones(5,length(t));
Ti= ones(5,length(t));
Tw= ones(5,length(t));
q=ones(5,length(t));
s=ones(5,length(t));

a = 20 ;                          %no of points
lambda_w= linspace(0.2,2,a); %thermal conductivity (W/mk)
                                  %sensitivity analysis
%%
for m = 1:1:a

%Properties of water
alpha_w(m) = lambda_w(m)/(Cp_w*rho_w);
%thermal diffusivity m/s^2;
Ste_i = Cp_i*( Tm-T2)/ L ; % stefan no for ice
Ste_w= Cp_w*( T1-Tm)/ L ; %stefan no for water

% calculating the constant of the soltuion
A = Ste_w*rho_w/rho_i;
B(m) = Ste_i*sqrt(alpha_i/alpha_w(m));
```

```
C = sqrt(pi);
D = @(p)p*alpha_i;
E = @(p)p*alpha_w(m);

X1= @(p)A.*exp(-p^2)./erf(p); %Liquid
X2= @(p)C.*p; %Latent Heat
X3= @(p)B(m)
.*exp(-p^2*(alpha_w(m)/alpha_i))./erfc(p*sqrt(alpha_w(m)/alpha_i));
%Solid

f1=@(p)(-X1(p)+ X2(p)- X3(p));
x0 = [0.1  20]; % initial interval
options = optimset('Display','iter'); % show iterations
[p(m), fval, exitflag, output] = fzero(f1,x0,options);

% constants for temperature profile :
Z(m) = (T2-Tm)/erfc(p(m)*sqrt(alpha_w(m)/alpha_i));
Q(m) = (Tm-T1)/erf(p(m));
d1 =length(t);

    for r=1:1:d1


    delta(m,r)= 2*p(m)*sqrt(alpha_w(m)*t(r)); % thickness in cm


    end
v(m)= delta(m,r); %final boundary position

%Now have to define x such that x --> delta for solid
% and delta <x--> for liquid
n=1:1:length(t);
y(m,n) = linspace(v(m),l,d1);
x(m,n) = linspace(0,v(m),d1);
x1(1:d1) = T1;
y1(m,1:d1) = T2;
t1=t(r);
    for n=1:1:length(t);
        q(m,n)=erf(x(m,n)/(2*sqrt(alpha_w(m)*t1)));
        Tw(m,n) = x1(n) + (Q(m)*q(m,n));
        thetaw(m,n) = (Tw(m,n)-T1)/(Tm-T1);
        %nondimensional temperature for water
        e(m,n) = (erfc(y(m,n)/(2*sqrt(alpha_i*t1))));
        Ti(m,n) = y1(m,n) - (Z(m).*e(m,n));
        thetai(m,n) = (Ti(m,n)-T2)/(Tm-T2);
        %nondimensional temperature for ice

        Fo(m,n) = alpha_i*t(n)/(l)^2; %fourier No
    end
```

```
end
Fo_1=Fo(n);
 Theta=horzcat(Tw,Ti);
 z=horzcat(x,y);

ddelta = zeros(1,a-1);
dlambda = zeros(1,a-1);
slope= zeros(1,a-1);

for m=1:1:a-1
    ddelta(1,m)= delta(m+1,r)-delta(m,r);
    dlambda(1,m)= lambda_w(1,m+1)-lambda_w(1,m);
    slope(1,m) = ddelta(1,m)/dlambda(1,m);
end
%%
xmarkers=0.6752 ;          %thermal conductivity (W/mk) of water.

figure(1)
plot((y(1,1:d1))/(l),thetai(1,1:d1),(y(2,1:d1))/(l),
thetai(2,1:d1),(y(3,1:d1))/(l),thetai(3,1:d1),(y(4,1:d1))/(l),
thetai(4,1:d1))
ylabel('\theta (Non dimensional temperature)')
xlabel('\sigma (x/L)')
title('Temperature profile for ice')
legend(sprintf('lambda_{w1}(%0.2f)',lambda_w(1)),
sprintf('lambda_{w2}(%0.2f)',lambda_w(2)),
sprintf('lambda_{w3}(%0.2f)',lambda_w(3)),
sprintf('lambda_{w4}(%0.2f)',lambda_w(4)),
sprintf('lambda_{w5}(%0.2f)',lambda_w(5)))

figure(2)
plot(t/60,delta(1,1:d1)/l,t/60,delta(2,1:d1)/l,
t/60,delta(3,1:d1)/l,t/60,delta(4,1:d1)/l,
t/60,delta(5,1:d1)/l)
xlabel('time (mins)')
ylabel('\delta/L')
title('Penetration depth for various stefan numbers')
legend(sprintf('lambda_{w1}(%0.2f)',lambda_w(1)),
sprintf('lambda_{w2}(%0.2f)',lambda_w(2)),
sprintf('lambda_{w3}(%0.2f)',lambda_w(3)),
sprintf('lambda_{w4}(%0.2f)',lambda_w(4)),
sprintf('lambda_{w5}(%0.2f)',lambda_w(5)))

figure(3)
plot(z(1,1:end),Theta(1,1:end), z(2,1:end),
Theta(2,1:end),z(3,1:end),
Theta(3,1:end),z(4,1:end),Theta(4,1:end),
z(4,1:end),Theta(4,1:end),
z(5,1:end),Theta(5,1:end))
ylabel('\theta (Non dimensional temperature)')
xlabel('\sigma (x/L)')
```

```
title('Temperature profile for ice')
legend(sprintf('lambda_{w1}(%0.2f)',lambda_w(1)),
sprintf('lambda_{w2}(%0.2f)',lambda_w(2)),
sprintf('lambda_{w3}(%0.2f)',
lambda_w(3)),sprintf('lambda_{w4}(%0.2f)',
lambda_w(4)),sprintf('lambda_{w5}(%0.2f)',lambda_w(5)))

figure(4)
[ax,p1,p2]= plotyy(lambda_w(2:a),slope,
lambda_w(2:a),delta(2:a,d1));
ylabel(ax(1),'\Delta \delta / \Delta \lambda ')
ylabel(ax(2),'\delta (m)')
xlabel(ax(1),'\lambda (W/mK)')
grid on
title ('Sensitivity of interface position (\delta)
v/s thermal conductivity (\lambda)')
legend('\Delta \delta / \Delta \lambda ','\delta')
```

A.2.3 Temperature Analysis

A common code for both temperature distribuio and Sensitivity Analysis.

```
% %
clear
clc
% Program to solve non dimensional analytical solution of the moving
% front problem
% ice and water as an example

%%
% studying the effect of temperature of ice:
% changing stefan no with changes in properties of ice

T1 = 95+273;   %Liquid temperature (K)
T2 = linspace(273-20,270,20);
%Solid Temperature (K) from -25 to -5 C
Tm = 0+273;    %Melting point of Solid (K)
l= 0.1; %Length of ice in solid in cm

%properties of water from data companion
R_w = [999.87,999.73,998.23,995.68,992.25,988.07,
983.23,977.93,971.82,965.34,958.38];
T_w = 273:10:373;

l_w = [0.552,0.607,0.641,0.665,0.682];
T_l =273:25:373 ;

Cp_1= [4221,4185.0,4181.6,4187.5,4199.6,4219.3];
T_cp =273:20:373;

L = 3.34*10^5;   %Latent heat of evaporation J/kg;
rho_w = interp1(T_w,R_w,T1);
```

```
Cp_w = interp1(T_cp,Cp_1,T1);
lambda_w =interp1(T_l,l_w,T1);
alpha_w= lambda_w./(Cp_w.*rho_w);

Ste_l= Cp_w*( T1-Tm)/ L ; %stefan no for water

a= length(T2);
%propeties of ice
%%
for m = 1:1:a
rho_i(m) = 917*(1- ((T2(m)-273)*1.17*10^-4));
%density of ice( T :celsius)
lambda_i(m) = 1.16*(1.91-(8.66*(10^-3)*T2(m))
+(2.97*(10^-5)*T2(m)^2));
% thermal conductivity W/mK
Cp_i(m) = (0.85+ (0.689*(10^-2)*T2(m)))*10^3;
%Heat capacity of ice J/kgK
alpha_i(m) = lambda_i(m)/(Cp_i(m)*rho_i(m));

Ste_i(m) = Cp_i(m)*(Tm-T2(m))/ L ; % stefan no for ice


% calculating the constant of the soltuion
A(m) = Ste_l*rho_w/rho_i(m);
B(m) = Ste_i(m)*sqrt(alpha_i(m)/alpha_w);
C = sqrt(pi);
D = @(p)p*alpha_i(m);
E = @(p)p*alpha_w;

X1= @(p)A(m).*exp(-p^2)./erf(p); %Liquid
X2= @(p)C.*p; %Latent Heat
X3= @(p)B(m)
.*exp(-p^2*(alpha_w/alpha_i(m))).*erfc(p*sqrt(alpha_w/alpha_i(m)));
%Solid

f1=@(p)(X1(p)- X2(p)- X3(p));
x0 = [0.1 20]; % initial interval
options = optimset('Display','iter'); % show iterations
[p(m), fval, exitflag, output] = fzero(f1,x0,options);

t=0:10:3000;


% constants for temperature profile :
Z(m) = (T2(m)-Tm)/erfc(p(m)*sqrt(alpha_w/alpha_i(m)));
Q(m) = (Tm-T1)/erf(p(m));
d1 =length(t);
    for r=1:1:d1


     delta(m,r)= 2*p(m)*sqrt(alpha_w*t(r)); % thickness in cm
```

```
    end
v(m)= delta(m,r); %final boundary position

%Now have to define x such that x --> delta for solid
% and delta <x--> for liquid
n=1:1:length(t);
y(m,n) = linspace(v(m),l,d1);
x(m,n) = linspace(0,v(m),d1);
x1(1:d1) = T1;
y1(m,1:d1) = T2(m);
t1=t(r);
    for n=1:1:length(t);
        q(m,n)=erf(x(m,n)/(2*sqrt(alpha_w*t1)));
        Tw(m,n) = x1(n) + (Q(m)*q(m,n));
        thetaw(m,n) = (Tw(m,n)-T1)/(Tm-T1);
        %nondimensional temperature
        e(m,n) = (erfc(y(m,n)/(2*sqrt(alpha_i(m)*t1))));
        Ti(m,n) = y1(m,n) - (Z(m).*e(m,n));
        thetai(m,n) = (Ti(m,n)-T2(1,m))/(Tm-T2(1,m));
        %nondimensional temperature

        Fo(m,n) = alpha_i(m)*t(n)/(l)^2;
        %fourier No
    end


end
Fo_1=Fo(n);
Theta=horzcat(Tw,Ti);
z=horzcat(x,y);

ddelta = zeros(1,a-1);
dT2 = zeros(1,a-1);
slope= zeros(1,a-1);

for m=1:1:a-1
    ddelta(1,m)= delta(m+1,r)-delta(m,r);
    dT2(1,m)= T2(1,m+1)-T2(1,m);
    slope(1,m) = ddelta(1,m)/(dT2(1,m));
end

figure(1)
plot((y(5,1:d1))/(l),thetai(5,1:d1),(y(12,1:d1))/(l),
thetai(12,1:d1),(y(20,1:d1))/(l),thetai(20,1:d1))
ylabel('\theta (Non dimensional temperature)')
xlabel('\sigma (x/L)')
title('Temperature profile for ice')
legend(sprintf('T2(%0.2f)',T2(5)),sprintf('T2(%0.2f)',
T2(12)),sprintf('T2(%0.2f)',T2(20)))
```

```
figure(2)
plot(Fo(1,1:d1),delta(1,1:d1)/l,Fo(2,1:d1),delta(2,1:d1)/l,
Fo(3,1:d1),delta(3,1:d1)/l,Fo(3,1:d1),delta(4,1:d1)/l)
xlabel('(fourier No)')
ylabel('\delta')
title('Penetration depth for various stefan numbers')
legend(sprintf('Ste_i(%0.2f)',Ste_i(1)),
sprintf('Ste_{i2}(%0.2f)',Ste_i(2)),sprintf('Ste_{i3}(%0.2f)',
Ste_i(3)),sprintf('Ste_{i4}(%0.2f)',Ste_i(4)))

figure(3)
plot(z(1,1:end),Theta(1,1:end), z(10,1:end),Theta(10,1:end),
z(20,1:end),Theta(20,1:end))
ylabel('temperature [K]')
xlabel('\sigma (x/l)')
title('Temperature profile for ice')
legend(sprintf('T2(%0.2f)',T2(1)),sprintf('T2(%0.2f)',
T2(10)),sprintf('T2(%0.2f)',T2(20)))

figure(4)
[ax,p1,p2]= plotyy(T2(2:a),slope,T2(2:a),delta(2:a,d1)/l);
ylabel(ax(1),'\Delta \delta / \Delta L ')
ylabel(ax(2),'\delta/l')
xlabel(ax(1),'Intial Temperature (T_2(K))')
p1.LineWidth = 2;
p2.LineWidth = 2;
grid(ax(1),'on')
title ( 'Sensitivity of interface position (\delta)
v/s Initial Temperature(T_2)')
legend('\Delta \delta / \Delta \lambda ','\delta',
sprintf('time (mins) =(%0.1f)',t(1,end)/60))
```

Bibliography

[1] Theodore R. Goodman and John J. SHEA. *The Melting of Finite Slabs*. 1960.

[2] C.F weaver et al. *Phase Equilibria in Molten Salt Breeder Reactor Fuels*. 1960.

[3] M. Richardson. *Development Of Freeze Valve For Use In The MSRE*. 1962.

[4] S.Cantor et al. *Physical Properties of Molten-Salt reactor Fuel, coolant and Flush Salts*. 1968.

[5] "Influence of natural convection on the melting process in a vertical cylindrical enclosure". In: *Letters in Heat and Mass Transfer* 7.5 (1980), pp. 329 –338.

[6] S.Fukusako. *Thermophysical Properties of Ice, Snow, and Sea Ice 1*. Plenum Publishing Corporation, 1990.

[7] Prof. Donald Sadoway. *Introduction to Solid State Chemistry, Lecture No: 10 Phase Equilibria and Phase Diagrams*. MIT Open CourseWare, 1993.

[8] M. Necati Özisik. *Heat Conduction, Second Edition*. JOHN WILEY & SONS, INC., 1993, pp. 392–436.

[9] R. Kahraman et al. *A simplified numerical model for melting of ice in a rectangular enclosure*. 1998.

[10] S.C. Gupta. *The Classical Stefan Problem Basic concepts, modelling, and analysis*. ELSEVIER SCIENCE B.V., 2003.

[11] L.P.B.M Janssen and M.M.C.G Warmoeskerken. *Transport Phenomena Data Companion*. VSSD, 2006.

[12] Linda Petzold et al. *Sensitivity Analysis of Differential- Algebraic Equations and Partial Difference Equations*. 2006.

[13] T.G. Myers et al. *A cubic heat balance integral method for one-dimensional melting of a finite thickness layer*. 2007.

[14] K.Hanjalic et al. *Analysis and Modelling of Physical Transport Phenomena*. VSSD, 2009, pp. 53–80.

[15] K.huffman. *Fukushima Daiichi Accident- Technical Causal Factor Analysis*. 2012.

[16] L.L.W. Frima. "Burnup in a Molten Salt Fast Reactor". MA thesis. Delft University of Technology, 2013.

[17] Jérôme Serp et al. "The molten salt reactor (MSR) in generation IV: Overview and perspectives". In: *Progress in Nuclear Energy* 77 (2014), pp. 308 –319.

[18] *World Nuclear Association*. URL: `http://www.world-nuclear.org/info/safety-and-security/safety-of-plants/fukushima-accident/`.